

lead to differences in the predicted stability of different conformers.

**Acknowledgment.** It is a pleasure to acknowledge Dr. M. Engel for modification to G-70 and helpful discussions. This work was supported in part by a grant from the U.S.-Israel Binational Science Foundation (A.T.H.).

## References and Notes

- (1) By structure we refer to bond distances and bond angles, whereas molecular conformation refers to the relationships between atoms separated by three or more bonds.
- (2) (a) B. J. Duke, *Theor. Chem.*, **2**, 159 (1975); (b) W. A. Lathan, L. A. Curtiss, W. J. Hehre, J. B. Lisle, and J. A. Pople, *Prog. Phys. Org. Chem.*, **11**, 175 (1974); (c) B. Pullman and A. Pullman, *Adv. Protein Chem.*, **28**, 347 (1974).
- (3) (a) *Pept.: Chem., Struct., Biol., Proc. Am. Pept. Symp., 4th, 1975*; (b) C. B. Anfinsen and H. A. Scheraga, *Adv. Protein Chem.*, **29**, 205 (1975); (c)

- A. T. Hagler and S. Lifson in "The Proteins", Academic Press, New York, N.Y., in press.
- (4) (a) H. Popkie, H. Kistenmacher, and E. Clementi, *J. Chem. Phys.*, **59**, 1325 (1973); (b) A. T. Hagler and A. Lapicciarella, *Biopolymers*, **15**, 1167 (1976).
  - (5) A. T. Hagler, L. Leiserowitz, and M. Tuval, *J. Am. Chem. Soc.*, **98**, 4600 (1976).
  - (6) W. J. Hehre, R. F. Stewart, and J. A. Pople, *J. Chem. Phys.*, **51**, 2657 (1969).
  - (7) Similar observations of this behavior with minimal basis sets in which cis conformations are calculated to be excessively stable have been noted previously in hydrocarbon systems.<sup>8-10</sup>
  - (8) L. Radom and J. A. Pople, *J. Am. Chem. Soc.*, **92**, 4786 (1970).
  - (9) W. J. Hehre, *J. Am. Chem. Soc.*, **94**, 6592 (1972).
  - (10) W. J. Hehre, *J. Am. Chem. Soc.*, **97**, 6941 (1975).
  - (11) W. J. Hehre, R. Ditchfield, and J. A. Pople, *J. Chem. Phys.*, **56**, 2 2257 (1972).
  - (12) A general discussion of the properties of the spatial distribution of electrons in amide, peptide, and carboxylic acid functional groups has been presented elsewhere: see ref. 4b.
  - (13) In the discussion here, when "the region surrounding the atom" is used it refers to the periphery of the molecule, away from the bonds, and not into the bonding region.

# Circular Dichroic Power Due to Chiral Exciton Coupling between Two Polyacene Chromophores

Nobuyuki Harada,\* Yuki Takuma, and Hisashi Uda

Contribution from Chemical Research Institute of Nonaqueous Solutions, Tohoku University, 2-1-1 Katahira, Sendai 980, Japan. Received October 31, 1977

**Abstract:** The CD spectra of (6*R*,15*R*)-(+)-6,15-dihydro-6,15-ethanonaphtho[2,3-*c*]pentaphene (**1**) and (7*R*,14*R*)-(+)-7,14-dihydro-7,14-ethanodibenz[*a,h*]anthracene (**2**) have been quantitatively calculated on the basis of a chiral exciton coupling mechanism between two anthracene or naphthalene chromophores. In the region of the allowed <sup>1</sup>B<sub>B</sub> transition which is polarized along the long axis of chromophores, the CD spectra were satisfactorily reproduced by the quantitative calculation using the UV data of component chromophores. The calculation results have established the absolute stereochemistries of these compounds in a nonempirical manner. The exciton analysis of UV spectra has confirmed the above assignments. The CD spectra of the <sup>1</sup>L<sub>a</sub> transition exhibit split Cotton effects of medium intensity, the sign of which has been explained by the point monopole approximation method. The calculation results have demonstrated the ideal examples of chiral exciton coupling and have established the unambiguity and reliability of the exciton chirality method.

In recent years, there has been a large amount of activity devoted to chiroptical properties of organic compounds which undergo chiral exciton coupling between two or more chromophores.<sup>1-6</sup> Namely, two identical or similar chromophores undergoing strong π-π\* transitions electrostatically interact with each other to exhibit two strong CD Cotton effects of opposite sign and of same rotational strength. Provided that two electric transition moments make positive exciton chirality, i.e., right-handed screwness, a positive CD Cotton effect at the longer wavelength side is observed together with a negative one at the shorter wavelength side.

In our previous papers,<sup>7-9</sup> we reported the synthesis and chiroptical properties of (6*R*,15*R*)-(+)-6,15-dihydro-6,15-ethanonaphtho[2,3-*c*]pentaphene (**1**) and (7*R*,14*R*)-(+)-7,14-dihydro-7,14-ethanodibenz[*a,h*]anthracene (**2**), the absolute configurations of which have been definitely determined by chemical correlations. These compounds exhibit very strong split CD Cotton effects due to the interaction between two anthracene or naphthalene chromophores. The results have demonstrated ideal cases of chiral exciton coupling in CD spectra, providing the most unambiguous evidence which demonstrates the consistency between nonempirical circular dichroic and x-ray Bijvoet methods.

The present CD exciton chirality method, which enables one to determine absolute configurations in a nonempirical manner, requires conservative Cotton effects of equal rotational

strength but of opposite sign. Namely, this method is applicable to the Cotton effects resulting only from the exciton coupling between two excitations (0 → a) of component chromophores without participation of other excited states (0 → b, etc.).<sup>10</sup> Therefore, for performing the reliable assignment of absolute stereochemistries by the CD method, it is important to choose the proper electronic transition of proper chromophores satisfying the following requirements of chiral exciton coupling: (1) large extinction coefficient values in UV spectra; (2) isolation of the band in question from other strong absorptions; (3) established direction of the electric transition moment in the geometry of the chromophore; (4) unambiguous determination of the exciton chirality in space, inclusive of configuration and conformation; and (5) negligible molecular orbital overlapping between the chromophores.

In the present paper, we wish to report the quantitative calculation results of CD spectra of these compounds, confirming the previously reported qualitative assignment.<sup>7-9</sup>

## Methods of Calculation

**Molecular Structure.** In the present calculation, the Cartesian coordinate systems for the molecular structures of compounds **1** and **2** are adopted as shown in Figure 1, in which the z axis is the C<sub>2</sub>-symmetrical axis of these molecules. Geometric parameters were taken from the x-ray crystallographic data of triptycene and 9,10-ethanoanthracene deriv-

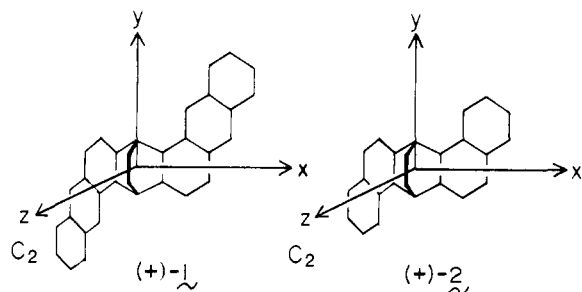


Figure 1. Cartesian coordinate systems for hydrocarbons (+)-1 and (+)-2.

atives;<sup>12</sup> aromatic C–C bond, 1.388 Å; benzylic C–C bond, 1.533 Å. Bond angles of  $sp^2$  and  $sp^3$  carbons are assumed to be  $120^\circ$  and  $109^\circ 28'$ , respectively. Namely, the dihedral angle between two anthracene or naphthalene chromophore planes is exactly  $120^\circ$ . The calculation of Cartesian coordinates was performed as follows: (1) the local axis  $x'$  was placed so that the  $yx'$  plane contains one of two anthracene planes, and the local coordinates of atoms contained in the  $yx'$  plane were calculated; (2) the principal coordinates were estimated as  $x = x' \cos 30^\circ$  and  $z = -x' \sin 30^\circ$ , while  $y$  coordinates remain unchanged. The Cartesian coordinates of the other anthracene plane and those of compound (+)-2 could be calculated in the same way.

**CD and UV Spectra.** The experimental dipole strength  $D$  was calculated from the observed UV spectrum by the equation

$$D = 9.184 \times 10^{-39} \int_0^\infty \epsilon(\sigma)/\sigma d\sigma \quad (\text{cgs unit}) \quad (1)$$

$$= \mu^2 = (er)^2$$

where  $\sigma$  is wavenumber,  $\mu$  is electric transition moment, and  $r$  is transition length. Similarly, the experimental rotational strength  $R$  is calculable from CD spectrum by the equations

$$R = 2.296 \times 10^{-39} \int_0^\infty \Delta\epsilon(\sigma)/\sigma d\sigma \quad (\text{cgs unit}) \quad (2)$$

$$= (2.296 \times 10^{-39}/\sigma_0) \int_0^\infty \Delta\epsilon(\sigma) d\sigma \quad (2a)$$

According to the molecular exciton theory,<sup>3b,11,13</sup> when  $N$  identical chromophores undergoing strong  $\pi-\pi^*$  transitions ( $0 \rightarrow a$ ) interact with each other, the excitation wavenumber  $\sigma_k$  to the  $k$ th excited level of the whole system is represented by the equation

$$\sigma_k - \sigma_0 = 2 \sum_{i=1}^N \sum_{j>i}^N C_{ik} C_{jk} V_{ij} \quad (3)$$

where  $\sigma_0$  is the excitation wavenumber of the isolated noninteracting chromophore,  $C_{ik}$  and  $C_{jk}$  are coefficients of the corresponding  $k$ th real wave function, and  $V_{ij}$  (expressed in  $\text{cm}^{-1}$  unit) is the transitional interaction energy between two chromophores  $i$  and  $j$ .

In a similar way, the  $k$ th rotational strength  $R^k$  and the dipole strength  $D^k$  due to the exciton coupling mechanism are expressed by eq 4 and 5, respectively,

$$R^k = -\pi\sigma_0 \sum_{i=1}^N \sum_{j>i}^N C_{ik} C_{jk} \mathbf{R}_{ij} \cdot (\boldsymbol{\mu}_{i0a} \times \boldsymbol{\mu}_{j0a}) \quad (4)$$

$$D^k = \left( \sum_{i=1}^N C_{ik} \boldsymbol{\mu}_{i0a} \right)^2 \quad (5)$$

where  $\mathbf{R}_{ij}$  is the interchromophoric distance vector from  $i$  to  $j$ , and  $\boldsymbol{\mu}_{i0a}$  and  $\boldsymbol{\mu}_{j0a}$  are electric transition moment vectors of groups  $i$  and  $j$ .

Table I. Exciton Chirality and Excitation Energy, Rotational Strength, and Dipole Strength of  $\alpha$  and  $\beta$  States of Binary Systems

Exciton chirality	$\mathbf{R}_{ij} \cdot (\boldsymbol{\mu}_{i0a} \times \boldsymbol{\mu}_{j0a}) V_{ij}$
$\alpha$ state	$\sigma_\alpha = \sigma_0 - V_{ij}$ $R^\alpha = (1/2)\pi\sigma_0 \mathbf{R}_{ij} \cdot (\boldsymbol{\mu}_{i0a} \times \boldsymbol{\mu}_{j0a})$ $D^\alpha = (1/2)(\boldsymbol{\mu}_{i0a} - \boldsymbol{\mu}_{j0a})^2$
$\beta$ state	$\sigma_\beta = \sigma_0 + V_{ij}$ $R^\beta = -(1/2)\pi\sigma_0 \mathbf{R}_{ij} \cdot (\boldsymbol{\mu}_{i0a} \times \boldsymbol{\mu}_{j0a})$ $D^\beta = (1/2)(\boldsymbol{\mu}_{i0a} + \boldsymbol{\mu}_{j0a})^2$

For binary systems ( $N = 2$ , groups  $i$  and  $j$ ) such as hydrocarbons (+)-1 and (+)-2, eq 3–5 are simplified as formulated in Table I, where states of  $k = 1$  and  $k = 2$  are denoted as  $\alpha$  and  $\beta$  states, respectively.<sup>14</sup>

The interaction energy  $V_{ij}$  is calculable by either the point dipole approximation method or the point monopole approximation method. By the point dipole approximation method, interaction energy is formulated as follows:

$$V_{ij} = \boldsymbol{\mu}_{i0a} \boldsymbol{\mu}_{j0a} \mathbf{R}_{ij}^{-3} (\mathbf{e}_i \cdot \mathbf{e}_j - 3(\mathbf{e}_i \cdot \mathbf{e}_{ij})(\mathbf{e}_j \cdot \mathbf{e}_{ij})) \quad (6)$$

where  $\mathbf{e}_i$ ,  $\mathbf{e}_j$ , and  $\mathbf{e}_{ij}$  are unit vectors of  $\boldsymbol{\mu}_{i0a}$ ,  $\boldsymbol{\mu}_{j0a}$ , and  $\mathbf{R}_{ij}$ , respectively, and the electric transition dipole moments  $\boldsymbol{\mu}_{i0a}$  and  $\boldsymbol{\mu}_{j0a}$  were estimated from the integrated peak area of the observed UV spectra.

By the point monopole approximation method, interaction energy is expressed as follows:

$$V_{ij} = 2 \sum_r \sum_s (C_{kr} C_{lr})_i (C_{ks} C_{ls})_j (rr/ss) \quad (7)$$

where  $r$  and  $s$  indicate atoms  $r$  and  $s$  in groups  $i$  and  $j$ , respectively, and  $k$  and  $l$  indicate occupied and vacant molecular orbitals regarding the excitation in each group, respectively. The electronic repulsion integral ( $rr/ss$ ) between two atoms  $r$  and  $s$  was estimated by the Nishimoto–Mataga equation.

In the actual calculation, eq 7 was not directly used. Instead, we have calculated the excitation energy levels by the Pariser–Parr–Pople molecular orbital method including configuration interaction between singly excited configurations (maximum 50 configurations). The following atomic orbital parameters were employed:  $W_C = -11.42$  eV,  $(rr/rr) = 10.84$  eV,  $\beta_{C-C}(\text{aromatic}) = -2.39$  eV. In the cases of compounds (+)-1 and (+)-2, the interatomic repulsion integral ( $rr/ss$ ) between two groups  $i$  and  $j$  was estimated only on the basis of distance, neglecting the angular factor. Similarly the resonance integrals  $\beta_{C-C}$  between two chromophores were completely neglected, which means that the molecular orbital overlapping between the two chromophores is negligible, and the interaction energy  $V_{ij}$  is mainly due to electrostatic interaction.

The actual CD spectrum curves  $\Delta\epsilon(\sigma)$  were calculated by the equation<sup>3b,15</sup>

$$\Delta\epsilon(\sigma) = \frac{1}{2.296 \times 10^{-39} \int_0^\infty f(\sigma)/\sigma d\sigma} \times \sum_{k=1}^N R^k f(\sigma + \sigma_0 - \sigma_k) \quad (8)$$

where  $f(\sigma)$  is the function describing the shape of a component CD Cotton effect curve ( $f(\sigma_0) = 1.0$ ) and was adopted from the actual UV spectrum of component chromophores. For binary systems ( $N = 2$ ), the states of  $k = \alpha$  and  $\beta$  are considered.

Numerical calculations were performed by using the computer ACOS series 77, NEAC 700 system of the Tohoku University Computer Center.

## Results and Discussion

**<sup>1</sup>B<sub>b</sub> Transition of Hydrocarbon (+)-1.** The CD and UV spectra due to the <sup>1</sup>B<sub>b</sub> transition of compound (+)-1 are shown

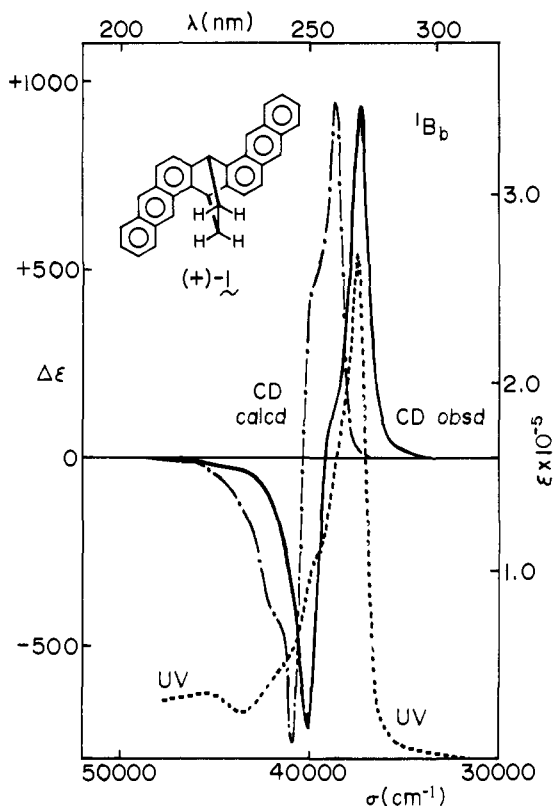


**Figure 2.** Calculated and observed CD and UV spectra due to the  ${}^1B_b$  transition of hydrocarbon (+)-**1**: (—), observed CD; (· · · · ·), calculated CD; (· · · · ·), observed UV.

in Figure 2. The UV spectrum exhibits an intense  ${}^1B_b$  absorption at 267.2 nm ( $\epsilon$  268 600) resembling the case of anthracene itself. Corresponding to the present absorption, the CD spectrum exhibits the very strong typical split Cotton effects (first Cotton effect,  $\Delta\epsilon_{268.0} = +931.3$ , and second Cotton effect,  $\Delta\epsilon_{249.7} = -720.8$ ;  $A (= \Delta\epsilon_1 - \Delta\epsilon_2) = +1652.1$ ), the positive sign of the  $A$  value being in accord with the positive exciton chirality between the two long axes of anthracene chromophores.

For the theoretical calculation of chiral exciton coupling in compound (+)-**1**, anthracene was adopted as the isolated and noninteracting component chromophore. From the UV spectrum of anthracene ( $\lambda_{\max}$  252 nm,  $\sigma_0 = 39\,682.5\text{ cm}^{-1}$ ,  $\epsilon$  204 000 in ethanol), transition length  $r$  was estimated by eq 1, giving  $r = 1.915\text{ \AA}$ . Since the  ${}^1B_b$  transition of anthracene is polarized along the long axis of the chromophore and anthracene is  $D_{2h}$  symmetrical, it is reasonable that the point dipole moment of the  ${}^1B_b$  transition is placed at the center of chromophores as illustrated in Figure 3.<sup>16</sup> In the original mode of coupling, since the two  ${}^1B_b$  transition moments are antiparallel to each other and are located at the center of the anthracene moieties, the electric interaction energy estimated by the point dipole approximation method is definitely positive. Actually, the value of  $V_{ij}$  calculated by eq 6 is  $+1130.9\text{ cm}^{-1}$ . This value is so large that the present exciton coupling belongs to the category of strong coupling. Since  $V_{ij}$  is positive, equations in Table I indicate that the  $\alpha$  state is located at longer wavelength side than the  $\beta$  state.

As illustrated in Figure 3, the hydrocarbon (+)-**1**, which is a cage compound of rigid molecular frame, is of  $C_2$  symmetry, having right-handed screwness between two  ${}^1B_b$  transition moments. Therefore the triple product  $\mathbf{R}_{ij} \cdot (\boldsymbol{\mu}_{i0a} \times \boldsymbol{\mu}_{j0a})$  is definitely positive; namely, the rotational strength of the  $\alpha$  state is positive, while that of the  $\beta$  state is necessarily negative. The numerical calculation of the theoretical rotational strength

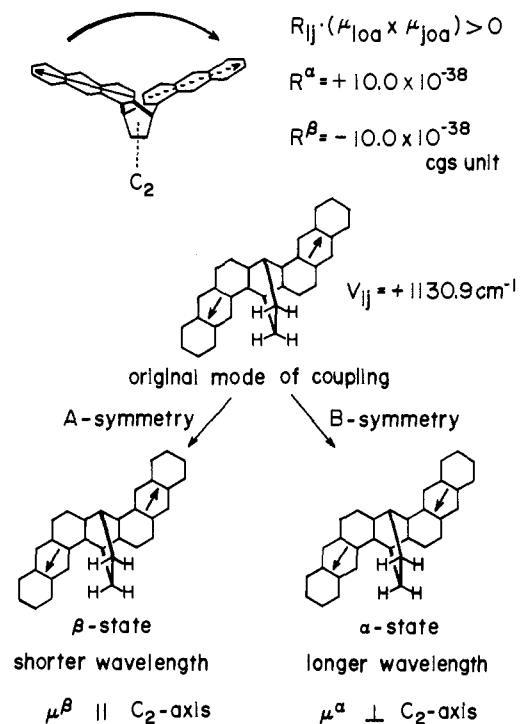


**Figure 3.** Rotational strength and coupling modes of two electric transition moments for the  ${}^1B_b$  transition of (+)-**1**.

formulated in Table I was performed by using the Cartesian coordinates of compound (+)-**1** and the UV spectral data, to give  $R^\alpha = +10.0 \times 10^{-38}$  and  $R^\beta = -10.0 \times 10^{-38}$  cgs unit.

As is well known, exciton chirality governing the sign and amplitude of split Cotton effects is defined by the quadruple product  $\mathbf{R}_{ij} \cdot (\boldsymbol{\mu}_{i0a} \times \boldsymbol{\mu}_{j0a}) V_{ij}$ . In the present case, since the quadruple product is of positive value, positive first and negative second Cotton effects are expected. The CD spectrum curve of compound (+)-**1** was numerically calculated by using eq 8 and the shape of the observed UV spectrum of anthracene (Figure 4); the calculated values of CD Cotton effects ( $\Delta\epsilon_{259} = +941.9$ ,  $\Delta\epsilon_{245} = -754.0$ ) are in excellent agreement with the observed values ( $\Delta\epsilon_{268} = +931.3$ ,  $\Delta\epsilon_{249.7} = -720.8$ , Figure 2). Namely, not only the sign but also the position, amplitude, and shape of the calculated Cotton effects agree with the observed one. Thus, the present results establish the ( $6R, 15R$ ) absolute stereochemistry of compound (+)-**1** in a nonempirical manner.<sup>18</sup>

The following analysis of the observed CD spectra confirms the above assignment. The rotational strengths of the observed apparent Cotton effects were calculated by eq 2a, giving  $R$  (first apparent Cotton)  $+7.43 \times 10^{-38}$  and  $R$  (second apparent Cotton)  $-7.53 \times 10^{-38}$  cgs unit, where the excitation wavenumber of anthracene,  $\sigma_0 = 39\,682.5\text{ cm}^{-1}$ , was employed (Table II). Thus, the observed Cotton effects exactly obey the sum rule ( $\Sigma R = 0$ ), which means that the present Cotton effects are based exclusively on the chiral exciton coupling between the two  ${}^1B_b$  transitions, without the participation of other  ${}^1L_a$  or  ${}^1L_b$  transitions. Namely, it is valid to employ only the conservative exciton coupling term in this case. In addition, the excellent agreement between the rotational strength values of theoretical apparent Cotton effects,  $R$  (first apparent Cotton)  $+7.73 \times 10^{-38}$  and  $R$  (second apparent Cotton)  $-7.80 \times 10^{-38}$ , and the observed values also supports the above assignment (Table II).<sup>19</sup>

The analysis of the UV spectrum also confirms the exciton coupling mechanism; as shown in Figure 3, the phase of two electric transition moments of  $\alpha$  state at the longer wavelength

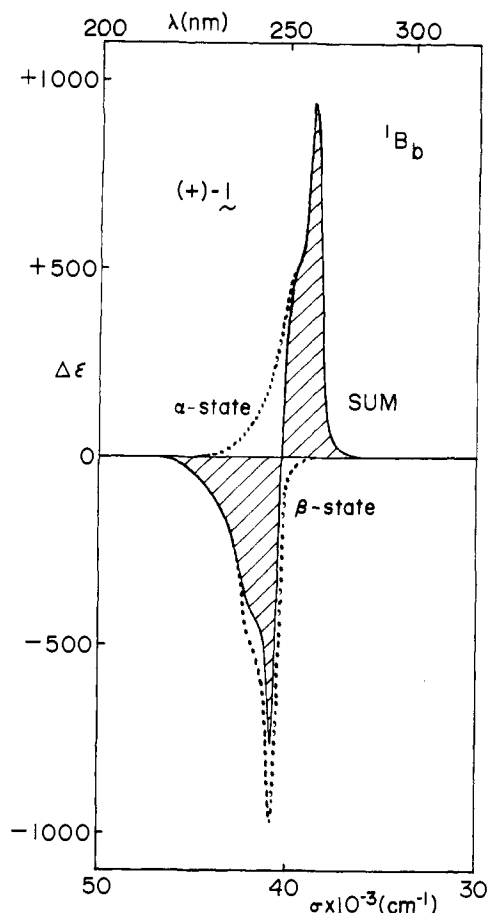


**Figure 4.** Summation of two component CD curves (· · · ·) taken from the shape of the UV spectrum of anthracene gives the calculated split CD Cotton effect curve (—) of compound (+)-1. Positive and negative shaded areas correspond to the calculated apparent rotational strengths of first and second Cotton effects, respectively (see Table II).

**Table II.** Spectral and Geometric Parameters and CD Cotton Effects Due to  ${}^1B_b$  Transition of Compounds (+)-1 and (+)-2

	(+)-1	(+)-2
Component chromophore	Anthracene	1,2-Dimethylnaphthalene
$\sigma_0$ , $\text{cm}^{-1}$	39 682.5	43 956.0
Transition length $r$ , Å	1.915	1.650
$R_{ij}$ , Å	7.689	5.808
$V_{ij}$ , $\text{cm}^{-1}$	+1130.9	+1060.7
Rotational strength $\times 10^{38}$ , cgs unit		
Theoretical	$R^\alpha + 10.0$ $R^\beta - 10.0$	$R^\alpha + 8.23$ $R^\beta - 8.23$
Theoretical apparent	$R_{1st} + 7.73$ $R_{2nd} - 7.80$	$R_{1st} + 4.41$ $R_{2nd} - 4.43$
Observed apparent	$R_{1st} + 7.43$ $R_{2nd} - 7.53$	$R_{1st} + 3.50$ $R_{2nd} - 1.70$
CD Cotton effects		
Calcd	$\Delta\epsilon_{259} = +941.9$ $\Delta\epsilon_{245} = -754.0$	$\Delta\epsilon_{233} = +470.9$ $\Delta\epsilon_{221} = -252.6$
Obsd	$\Delta\epsilon_{268} = +931.3$ $\Delta\epsilon_{249.7} = -720.8$	$\Delta\epsilon_{237} = +326.5$ $\Delta\epsilon_{224} = -180.5$

side is in phase, while that of  $\beta$  state at shorter wavelength side is out of phase. Since the angle between two vectors is  $151.0^\circ$ , the in-phase combination of electric transition moments results in a larger resultant moment than that of the out-of-phase combination (Figure 5). The calculated ratio of two dipole strengths is  $D^\alpha:D^\beta = 15:1$ . Thus the theoretical calculation based on the exciton coupling mechanism predicts that the UV intensity at the longer wavelength side is stronger than that at

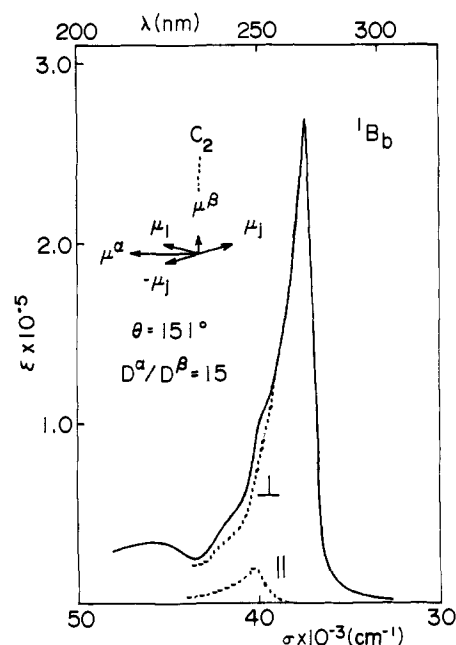


**Figure 5.** Calculated divided spectra of the  ${}^1B_b$  transition of hydrocarbon (+)-1. Symbols  $\perp$  and  $\parallel$  indicate the absorption perpendicular and parallel to the  $C_2$  axis, respectively. Since the angle  $\theta$  between two moments is  $151.0^\circ$ , the ratio  $\mu^\alpha/\mu^\beta$  is  $\sqrt{15}$ , therefore  $D^\alpha/D^\beta = 15$ : (—), observed UV; (· · · ·), divided spectra.

the shorter wavelength side. In other words, the UV peak is shifted to the side of the first Cotton effect at the longer wavelength side. The observed UV spectrum provides a striking confirmation of this effect; the UV maximum peak is located at  $37\,425.1\text{ cm}^{-1}$ , being closer to the first Cotton effect at  $37\,313.4\text{ cm}^{-1}$  than to the second one at  $40\,048.0\text{ cm}^{-1}$  (Figure 2). From the  $C_2$ -symmetrical properties, the transition of the  $\beta$  state (A symmetry) is polarized along the  $C_2$  axis, while the transition moment of the  $\alpha$  state (B symmetry) is perpendicular to the axis (Figure 5 and Table III).

The observed UV spectrum was actually divided, in the ratio of 15:1, into two component transitions of  $\alpha$  and  $\beta$  states, as shown in Figure 5. By this analysis, it is likely that the shoulder around 250 nm is due to the weak transition of the  $\beta$  state. Thus, the shape of the UV spectrum is explicable by the simple exciton coupling mechanism.

As indicated by eq 7, the interaction energy  $V_{ij}$  is also calculable by the point monopole approximation method. The theoretical value of  $V_{ij}$  calculated by the SCF-CI molecular orbital method is  $+638.7\text{ cm}^{-1}$ , which is about one-half of the value obtained by the point dipole approximation method (Tables II and III). Therefore, if this value is adopted as the  $V_{ij}$  value, the amplitude of calculated Cotton effects becomes smaller. However, by combining the present  $V_{ij}$  value with the theoretically calculated value of transition length  $r = 2.505\text{ Å}$ , the split Cotton effects of  $\Delta\epsilon_{256} = +1609$  and of  $\Delta\epsilon_{248} = -836$  were obtained. Thus, the SCF-CI molecular orbital calculations also give reasonable results.

The qualitative point monopole treatments on the basis of the Platt's polarization diagram are visualized in Figure 6. The  $\alpha$  state of B symmetry is more stable than the  $\beta$  state of A symmetry, because in the  $\alpha$  state, the plus and minus regions are close to each other. Thus, the positive value of interaction energy  $V_{ij}$  is established even by the qualitative Platt's polarization diagram, and there is no doubt of the assignment of CD and UV spectra of the  ${}^1B_b$  transition of compound (+)-1. After all the (6R,15R) absolute stereochemistry of compound (+)-1 is unambiguously established on the basis of the chiral exciton coupling mechanism of the split Cotton effects.

Table III. SCF-CI Calculation Results<sup>a</sup> of Anthracene and Hydrocarbon (+)-1

Compd	Transition	Excitation energy, cm <sup>-1</sup>	Oscillator strength (f)	Polarization	Symmetry	$\sigma_A - \sigma_B$ , cm <sup>-1</sup>	
Anthracene	<sup>1</sup> L <sub>a</sub>	27 698.5	0.304	Short			
	<sup>1</sup> L <sub>b</sub>	29 865.0	0.0				
	<sup>1</sup> B <sub>b</sub>	40 738.1	2.774	Long			
(+) -1	<sup>1</sup> L <sub>a</sub>	28 081.9	0.120	<sup>b</sup>	A	-182.6	
		28 264.5	0.588	⊥	B		
	<sup>1</sup> L <sub>b</sub>	31 446.5	0.0				
		31 446.5	0.0				
	<sup>1</sup> B <sub>b</sub>	38 699.6	0.383	⊥	B		+226.0
		38 925.6	0.011		A		
		40 633.8	4.484	⊥	B		
	<sup>1</sup> B <sub>b</sub>	41 911.1	0.293		A	+1277.4	

<sup>a</sup> Configuration interactions between 49 and 50 singly excited configurations were calculated for anthracene and (+)-1, respectively. <sup>b</sup> Symbols || and ⊥ indicate the polarization of transitions parallel and perpendicular to the C<sub>2</sub> axis, respectively.

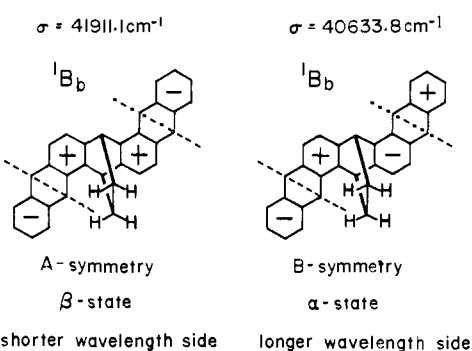


Figure 6. The point monopole treatments of the <sup>1</sup>B<sub>b</sub> transition of hydrocarbon (+)-1, on the basis of the Platt's polarization diagram.

**<sup>1</sup>B<sub>b</sub> Transition of Hydrocarbon (+)-2.** The UV spectrum of compound (+)-2 shows the <sup>1</sup>B<sub>b</sub> transition at 232.3 nm ( $\epsilon$  98 200), corresponding to which the CD spectrum exhibits typical strong split Cotton effects ( $\Delta\epsilon_{237.0} = +326.5$ ,  $\Delta\epsilon_{224.0} = -180.5$ ;  $A = +507.0$ , Figure 7). Besides the split Cotton effects, the third Cotton effect of negative sign is observed at 205 nm ( $\Delta\epsilon_{205} = -115.0$ ). As in the case of compound (+)-1, since the sign of the  $A$  value is positive, the positive exciton chirality between the two long axes of naphthalene chromophores is assigned to (+)-2. Namely, the (7*R*,14*R*) absolute configuration of (+)-2 is established.

The CD spectrum was quantitatively calculated using the UV spectral data of 1,2-dimethylnaphthalene (see Table II and Figure 7). Although the calculated amplitude is larger than the observed value, the sign and position of Cotton effects are in good agreement with the observed ones.

The experimental apparent rotational strengths derived from the integrated peak area of positive first and negative second Cotton effects are  $R$  (first) =  $+3.50 \times 10^{-38}$  and  $R$  (second) =  $-1.70 \times 10^{-38}$  cgs unit. The theoretical apparent rotational strengths were calculated in the same way as in the case of compound (+)-1, giving  $R$  (first) =  $+4.41 \times 10^{-38}$  and  $R$  (second) =  $-4.43 \times 10^{-38}$  cgs unit (Table II). The experimental and theoretical values of the first Cotton effect almost agree with each other, while the experimental value of the second Cotton effect is relatively smaller than the theoretical one. The discrepancy between the observed and calculated values of the second Cotton effect is presumably due to the fact that the second Cotton effect overlaps with the third transition below 220 nm, which probably couples with the present <sup>1</sup>B<sub>b</sub> transition to some extent. For example, in the cases of dimethyl and tetramethyl derivatives of (+)-2, the second Cotton effect becomes weaker, while the third one becomes stronger.<sup>9</sup>

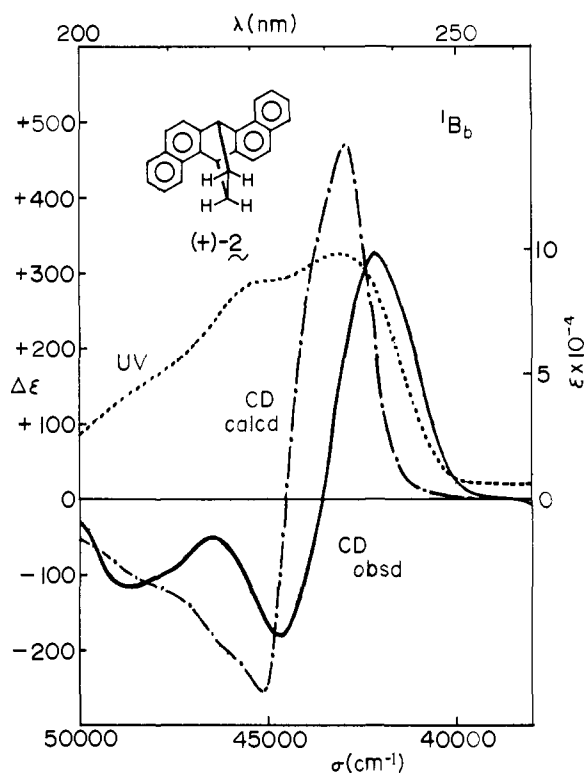


Figure 7. CD and UV spectra of compound (+)-2 at the region of <sup>1</sup>B<sub>b</sub> transition: (—), observed CD; (- - - - -), calculated CD; (· · · · ·), observed UV.

The analysis of the asymmetrical pattern of the observed UV spectrum and the SCF-CI molecular orbital calculation support the present interpretation based on the exciton coupling mechanism, as in the case of compound (+)-1. Namely, the position of the UV peak is closer to the first Cotton effect than to the second one, as expected from the theoretical results, and the value  $\sigma_A - \sigma_B (= 2V_{ij})$  calculated by the SCF-CI method is  $+546.2$  cm<sup>-1</sup>, indicating that the  $\alpha$  state of B symmetry is more stable than the  $\beta$  state of A symmetry (Table IV). Thus, the (7*R*,14*R*) absolute configuration of compound (+)-2 was definitely established on the basis of the chiral exciton coupling mechanism.

**<sup>1</sup>L<sub>a</sub> Transition of Hydrocarbon (+)-1.** Unlike the case of the intense <sup>1</sup>B<sub>b</sub> transition, the CD spectrum of compound (+)-1 due to the <sup>1</sup>L<sub>a</sub> transition exhibits Cotton effects of medium intensity showing the complicated vibrational structures as shown in Figure 8 ( $\Delta\epsilon_{397.2} = +26.4$ ,  $\Delta\epsilon_{388.1} = -2.3$ ,  $\Delta\epsilon_{378.0} =$

**Table IV.** SCF-CI Calculation Results<sup>a</sup> of Naphthalene and Hydrocarbon (+)-2

Compd	Transition	Excitation energy, cm <sup>-1</sup>	Oscillator strength ( <i>f</i> )	Polarization	Symmetry	$\sigma_A - \sigma_B$ , cm <sup>-1</sup>
Naphthalene	<sup>1</sup> L <sub>b</sub>	33 367.8	0.0			
	<sup>1</sup> L <sub>a</sub>	35 803.7	0.247	Short		
	<sup>1</sup> B <sub>b</sub>	46 451.1	2.027	Long		
(+) -2	<sup>1</sup> L <sub>b</sub>	{ 34 156.5 34 156.5	{ 0.0 0.0			
	<sup>1</sup> L <sub>a</sub>	{ 35 821.7 35 990.6	{ 0.075 0.424	<i>b</i> ⊥	A B	-169.0
	<sup>1</sup> B <sub>b</sub>	{ 45 915.7 46 461.9	{ 3.462 0.173	⊥ 	B A	+546.2

<sup>a</sup> Configuration interactions between 25 and 50 singly excited configurations were calculated for naphthalene and (+)-2, respectively. <sup>b</sup> See footnote b, Table III.

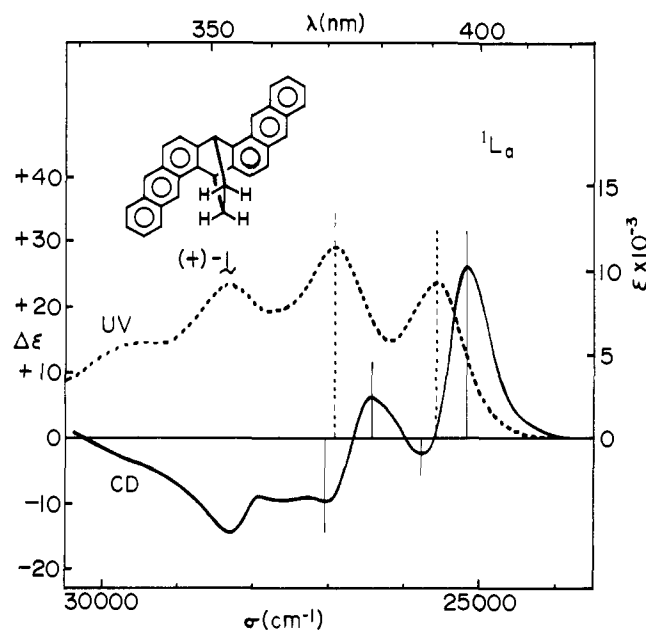


**Figure 8.** CD and UV spectra of compound (+)-1 at the region of <sup>1</sup>L<sub>a</sub> transition: (—), observed CD; (·····), observed UV.

+6.3,  $\Delta\epsilon_{370.0} = -9.7$ ,  $\Delta\epsilon_{362.9} = -9.7$ ,  $\Delta\epsilon_{352.8} = -14.5$ ). In the spectra, the first UV vibrational peak splits into two CD Cotton effects of opposite sign to each other, and the order of sign is positive and negative from the longer wavelength side. The same is true for the second UV vibrational peak. In addition, the shape of the whole Cotton effects is positive at the longer wavelength side and negative at the shorter wavelength side. The apparent rotational strengths of the positive and negative areas of the Cotton effects are similar to each other, except for their signs; the observed apparent rotational strengths are  $R$  (positive area) =  $+1.67 \times 10^{-39}$  and  $R$  (negative area) =  $-2.38 \times 10^{-39}$  cgs unit, where  $\sigma_0 = 26\,702.2$  cm<sup>-1</sup>, the wavenumber of a zero-line intersection, was used. Therefore it is probable that the chiral exciton coupling between two <sup>1</sup>L<sub>a</sub> transition moments results in these split Cotton effects. Since each UV vibrational peak shows exciton splitting, these Cotton effects belong to the category of weak exciton coupling.

Since the <sup>1</sup>L<sub>a</sub> transition of anthracene is polarized along the short axis of the chromophore (Table III and Figure 9) and the molecular frame of this cage compound is very rigid, the triple product  $\mathbf{R}_{ij} \cdot (\boldsymbol{\mu}_{i0a} \times \boldsymbol{\mu}_{j0a})$  is unambiguously of negative value (Figure 9). Therefore the remaining problem is whether the interaction energy  $V_{ij}$  is positive or negative. It is, however, difficult to predict the sign of the  $V_{ij}$  value without quantitative calculations in this case, in contrast to the case of the <sup>1</sup>B<sub>b</sub>

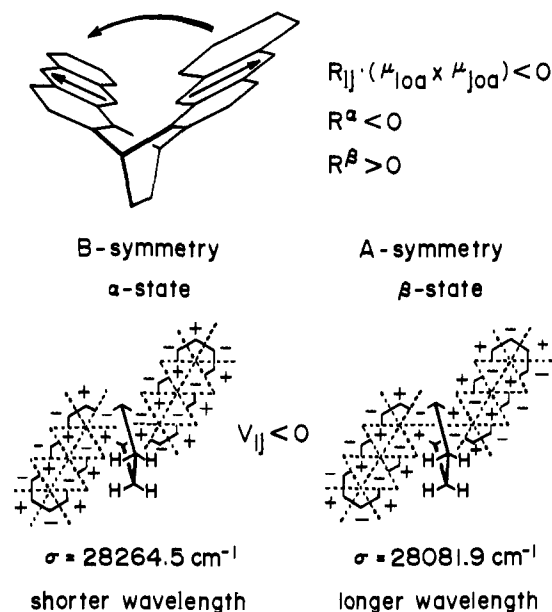


**Figure 9.** Rotational strength and point monopole approximation of the coupled <sup>1</sup>L<sub>a</sub> transitions of hydrocarbon (+)-1.

transition of compounds (+)-1 and (+)-2. When interaction energy was estimated by the point dipole approximation, a small negative value was obtained ( $V_{ij} = -18.5$  cm<sup>-1</sup>, Table V). By the point monopole approximation method, i.e., by the SCF-CI molecular orbital method, the calculated  $V_{ij}$  value is  $-91.3$  cm<sup>-1</sup>. Therefore, the quadruple product  $\mathbf{R}_{ij} \cdot (\boldsymbol{\mu}_{i0a} \times \boldsymbol{\mu}_{j0a}) V_{ij}$  of positive value is concluded. Thus, the observed order of the sign of split Cotton effects is explainable by either the point monopole or point dipole approximation methods. The qualitative point monopole approximation is visualized by the Platt's polarization diagram in Figure 9; in the present case, the local polarizations favor the  $\beta$  state of A symmetry.

The circular dichroism curve of the <sup>1</sup>L<sub>a</sub> transition of compound (+)-1 was numerically calculated using the UV spectral data of anthracene (Table V). Since the  $V_{ij}$  value depends on the approximation methods used, the computation was performed for various  $V_{ij}$  values. In Figure 10, three resultant curves are depicted ( $V_{ij} = -18.5$ ,  $-40.0$ , and  $-91.3$  cm<sup>-1</sup>). Each UV vibrational peak splits into two CD Cotton effects of opposite sign and the order of the sign is plus/minus/plus/minus from the longer wavelength side. Thus the calculated sign of split Cotton effects of at least the first two UV vibrational peaks agrees with the observed one. The calculated CD amplitude by the point dipole approximation ( $V_{ij} = -18.5$  cm<sup>-1</sup>) is smaller than the observed one, while that by the point monopole approximation ( $V_{ij} = -91.3$  cm<sup>-1</sup>) is too large

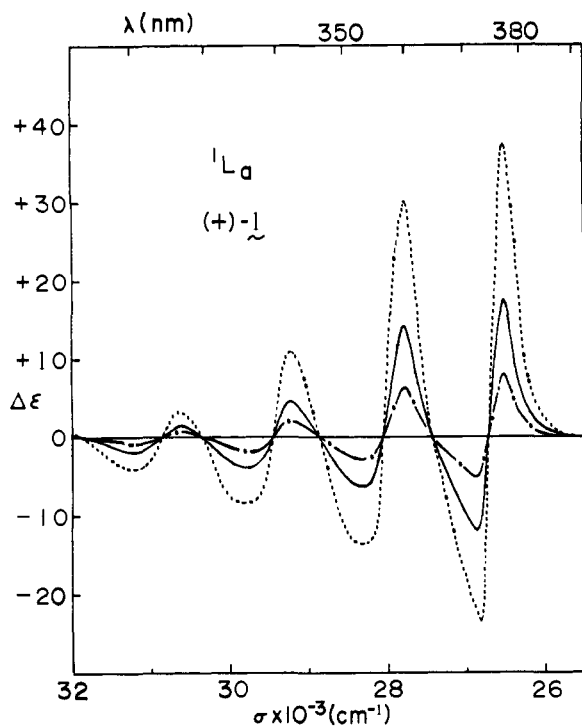


Figure 10. Calculated CD spectra of the  ${}^1L_a$  transition of hydrocarbon (+)-1: (.....),  $V_{ij} = -91.3 \text{ cm}^{-1}$ ; (—),  $V_{ij} = -40.0 \text{ cm}^{-1}$ ; (- · · · · ·),  $V_{ij} = -18.6 \text{ cm}^{-1}$ .

(Figure 10). Since the curve of  $V_{ij} = -40 \text{ cm}^{-1}$  fits the observed curve, the actual interaction energy is approximated by this value.

Despite the good agreement between the signs of theoretical and experimental Cotton effects, the shape of the calculated split Cotton effects, especially that of the shorter wavelength part, is different from the observed one. Namely, the calculated curve exhibits typical oscillation, while the observed one shows two main broad Cotton effects accompanied with oscillation of small amplitude. It is likely that the present discrepancy between the shape of these two curves is attributable to broadening of UV vibrational peaks by exciton coupling, and also to the participation of other transitions.<sup>20</sup>

The position of the theoretical Cotton effects is shifted by  $1300 \text{ cm}^{-1}$  to the shorter wavelength side from the observed one. This disagreement is due to the adoption of anthracene as the component chromophore, because the excitation energy of the  ${}^1L_a$  transition of unsubstituted anthracene is ca.  $1100 \text{ cm}^{-1}$  higher than that of compound **1**.

The assignment of the CD spectrum on the basis of exciton coupling is supported by the analysis of the UV spectrum. Unlike the case of the  ${}^1B_b$  transition, the transition of A symmetry is located at the longer wavelength side, being polarized along the  $C_2$  axis (Table III). Since the angle between the two short axes is  $128.7^\circ$ , the UV dipole strength of the B symmetrical transition at the shorter wavelength side is larger than that of the A-symmetrical one at the longer wavelength side; the calculated ratio of dipole strength is 4.33. In fact, the observed maxima of two UV vibrational peaks are closer to the second Cotton effects than to the first ones, respectively: for the first UV vibrational peak at  $25\,575.4 \text{ cm}^{-1}$ ,  $\sigma$  (first Cotton) =  $25\,176.2 \text{ cm}^{-1}$  and  $\sigma$  (second Cotton) =  $25\,766.5 \text{ cm}^{-1}$ ; for the second peak at  $26\,939.6 \text{ cm}^{-1}$ ,  $\sigma$  (first) =  $26\,455.0 \text{ cm}^{-1}$  and  $\sigma$  (second) =  $27\,027.0 \text{ cm}^{-1}$  (Figure 8). However, because of the small values of energy splitting, the present assignment of the UV spectrum based on the exciton coupling mechanism is not so reliable as in the case of the  ${}^1B_b$  transition.

**${}^1L_a$  Transition of Hydrocarbon (+)-2.** The CD and UV

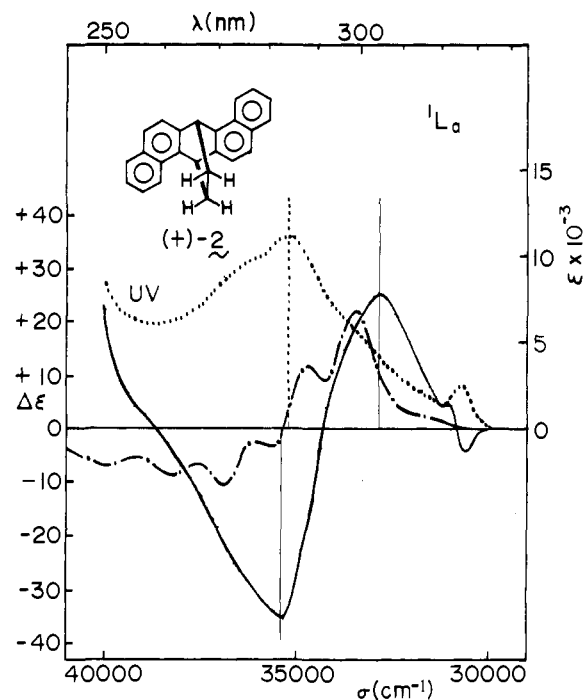


Figure 11. CD and UV spectra due to the  ${}^1L_a$  transition of hydrocarbon (+)-2: (—), observed CD; (- · · · · ·), calculated CD; (.....), observed UV.

Table V. Spectral and Geometric Parameters for the  ${}^1L_a$  Transition of Compounds (+)-1 and (+)-2

	(+)-1	(+)-2
Component chromophore	Anthracene	1,2-Dimethylnaphthalene
$\sigma_0, \text{ cm}^{-1}$	28 089.8	35 211.2
Transition length $r, \text{ \AA}$	0.553	0.570
$R_{ij}, \text{ \AA}$	7.689	5.808
Rotational strength $\times 10^{38}, \text{ cgs unit}$		
Theoretical	$R^\beta + 1.716$ $R^\alpha - 1.716$	$R^\beta + 1.537$ $R^\alpha - 1.537$
Observed apparent	$R_{\text{positive area}} + 0.167$ $R_{\text{negative area}} - 0.238$	$R_{1st} + 0.338$ $R_{2nd} - 0.559$
$V_{ij}, \text{ cm}^{-1}$		
By point dipole	-18.5	+36.5
By point monopole	-91.3	-84.5

spectra of the  ${}^1L_a$  transition of hydrocarbon (+)-2 are shown in Figure 11. Unlike the case of hydrocarbon (+)-1, the UV spectrum exhibits a broad peak of medium intensity ( $\lambda_{\text{max}} 283.5 \text{ nm}$ ,  $\epsilon 11\,100$ ). The CD spectrum shows two split Cotton effects which are positive at the longer wavelength side and negative at the shorter wavelength side. Since the rotational strengths of the observed apparent Cotton effects are similar to each other ( $R$  (first) =  $+3.38 \times 10^{-39}$ ,  $R$  (second) =  $-5.59 \times 10^{-39}$  cgs unit), it is probable that these Cotton effects are due to the exciton coupling between two short-axis-polarized  ${}^1L_a$  transitions. However, the observed pattern of CD Cotton effects disagrees with that expected from the point dipole approximation, but is consistent with that by the point monopole approximation method (Table V). Namely, the triple product  $R_{ij}(\mu_{i0a} \times \mu_{j0a})$  is negative, while  $V_{ij}$  by the SCF-CI calculation is positive (Table V). Since the quadruple product is positive, the positive first and negative second Cotton effects are assigned in consistency with the observed pattern.

The CD spectrum was numerically calculated in the same way as in the case of compound **1**. Even the amplitude calculated with the  $V_{ij}$  value of  $-84.5 \text{ cm}^{-1}$  by the point monopole

approximation is quite smaller than the observed one. Therefore the  $V_{ij}$  value was arbitrarily increased, and a similar amplitude to the observed one was obtained when the  $V_{ij}$  value was  $-400 \text{ cm}^{-1}$  (Figure 11). Thus, although the calculation of the shape and amplitude of the Cotton effects is insufficient, the sign of the Cotton effects is explicable by the point monopole approximation method.

The analysis of the pattern of the UV spectrum supports the exciton coupling mechanism, as in the case of hydrocarbon (+)-1. Namely, the UV dipole strength of the  $\beta$  state at the longer wavelength side is smaller than that of the  $\alpha$  state at the shorter wavelength side. This situation is in accord with the pattern of the observed UV spectrum (Figure 11 and Table IV).

**$^1L_b$  Transition of Hydrocarbon (+)-2.** In the case of hydrocarbon (+)-1, the weak  $^1L_b$  transition buried in the  $^1L_a$  transition was not detected in both UV and CD spectra. On the other hand, the hydrocarbon (+)-2 exhibits very weak negative and positive Cotton effects around 330 nm (Figure 11). However, since the amplitude of UV and CD spectra is quite small, it is not appropriate to apply the chiral exciton coupling mechanism to the present  $^1L_b$  transition.

## Conclusions

The present CD calculation results on the asymmetrical rigid cage compounds have not only demonstrated the ideal examples of chiral exciton coupling, but also established the unambiguity and reliability of the exciton chirality method for determining absolute stereochemistries of optically active compounds. As seen in the present results, for determining absolute stereochemistry by the CD exciton method, it is important to choose the proper transition of proper chromophores which satisfy the requirements of chiral exciton coupling.

**Acknowledgments.** The authors thank Professor Stephen F. Mason for valuable comments. The present work was partially supported by a Grant-in-Aid for Scientific Research from the Ministry of Education of Japan.

## References and Notes

- S. F. Mason, *J. Chem. Soc., Chem. Commun.*, 239 (1973); S. F. Mason, R. H. Seal, and D. R. Roberts, *Tetrahedron*, **30**, 1671 (1974), and references cited therein.
- I. Hanazaki and H. Akimoto, *J. Am. Chem. Soc.*, **94**, 4102 (1972), and references cited therein.
- (a) N. Harada and K. Nakanishi, *Acc. Chem. Res.*, **5**, 257 (1972); (b) N. Harada, S. L. Chen, and K. Nakanishi, *J. Am. Chem. Soc.*, **97**, 5345 (1975); (c) N. Harada, N. Ochiai, K. Takada, and H. Uda, *J. Chem. Soc., Chem. Commun.*, 495 (1977), and references cited therein.
- S. Hagishita and K. Kuriyama, *Tetrahedron*, **28**, 1435 (1972), and references cited therein.
- J. Tanaka, C. Katayama, F. Ogura, H. Tatemitsu, and M. Nakagawa, *J. Chem. Soc., Chem. Commun.*, 21 (1973); M. Hashimoto, Y. Shimizu, F. Ogura, and M. Nakagawa, *Bull. Chem. Soc. Jpn.*, **47**, 1761 (1974); A. Kaito, A. Tajiri, M. Hatano, F. Ogura, and M. Nakagawa, *J. Am. Chem. Soc.*, **98**, 7932 (1976), and references cited therein.
- A. M. F. Hezemans and M. P. Groenewege, *Tetrahedron*, **29**, 1223 (1973).
- N. Harada, Y. Takuma, and H. Uda, *J. Am. Chem. Soc.*, **98**, 5408 (1976).
- N. Harada, Y. Takuma, and H. Uda, *Bull. Chem. Soc. Jpn.*, **50**, 2033 (1977).
- N. Harada, Y. Takuma, and H. Uda, *Bull. Chem. Soc. Jpn.*, **51**, 265 (1978).
- Tinoco has derived the equations for the rotational strength of the transition ( $0 \rightarrow a$ ), including the contribution of other excited states ( $0 \rightarrow b$ , etc.).<sup>11</sup>

The use of the first term of the equation, i.e., a conservative term, permits unambiguous assignments of absolute stereochemistries, provided that the second and higher terms of the equation are negligible. The conditions described in the introduction are necessary for ignoring the higher terms.

- I. Tinoco, Jr., *Adv. Chem. Phys.*, **4**, 113 (1962); "Fundamental Aspects and Recent Developments in Optical Rotatory Dispersion and Circular Dichroism", F. Ciardelli and P. Salvadori, Ed., Heyden, London, 1973, Chapter 2.4.
- N. Sakabe, K. Sakabe, K. Ozeki-Minakata, and J. Tanaka, *Acta Crystallogr., Sect. B*, **28**, 3441 (1972).
- I. Tinoco, Jr., R. W. Woody, and D. F. Bradley, *J. Chem. Phys.*, **38**, 1317 (1963).
- The  $\alpha$  and  $\beta$  states correspond to the  $-$  and  $+$  states denoted in ref 11, respectively.
- Equation 8 can be modified as follows:

$$\Delta\epsilon(\sigma) = \frac{\sigma_0}{2.296 \times 10^{-39}} \int_0^\infty f\left(\frac{\sigma - \sigma_0}{\Delta\sigma}\right) d\sigma \sum_{k=1}^N R^k f\left(\frac{\sigma - \sigma_k}{\Delta\sigma}\right) \quad (9)$$

where  $f[(\sigma - \sigma_0)/\Delta\sigma]$  is the function describing the shape of actual UV ( $f(0) = 1.0$ ) and  $\Delta\sigma$  is an arbitrary value. When  $f[(\sigma - \sigma_0)/\Delta\sigma]$  is approximated by the Gaussian distribution,  $\Delta\sigma$  is the standard deviation. The Taylor expansion of eq 9 gives eq 10 as the second term:

$$\Delta\epsilon(\sigma) = \frac{-\sigma_0 f^{(1)}\left(\frac{\sigma - \sigma_0}{\Delta\sigma}\right)}{2.296 \times 10^{-39}} \int_0^\infty f\left(\frac{\sigma - \sigma_0}{\Delta\sigma}\right) d\sigma \sum_{k=1}^N R^k \left(\frac{\sigma_k - \sigma_0}{\Delta\sigma}\right) \quad (10)$$

where  $f^{(1)}[(\sigma - \sigma_0)/\Delta\sigma]$  indicates the value of  $d/dx f(x)$  when  $x = (\sigma - \sigma_0)/\Delta\sigma$ . The first term of the expansion is zero, and other higher terms are negligible because of  $(\sigma_k - \sigma_0)/\Delta\sigma \ll 1$ . In addition, in the case of binary systems ( $N = 2$ ), all the odd terms vanish on the basis of the sum rule ( $\sum_{k=1}^N R^k = 0$ ). Since the values  $R^k$  and  $\sigma_k - \sigma_0$  are expressed by eq 3 and 4, the exciton chirality of binary systems is quantitatively defined by the quadruple product  $\mathbf{R}_i(\mu_{j0a} \times \mu_{j0b})V_{ij}$ . In the present studies, the direct summation method by eq 8 was employed for the sake of simplicity.

- As indicated by eq 4, the rotational strength due to chiral exciton coupling is origin independent. Therefore it is important to determine the place of the point dipole in the chromophore. In the cases of anthracene and naphthalene, it is reasonable to place the point dipole at the center of the chromophore because of the symmetrical properties and the following dipole velocity treatment; the magnetic transition moment is expressed by<sup>17</sup>

$$\langle \Phi_0 | \mathbf{r} \times \nabla | \Phi_a \rangle = \sum_{\text{all bonds}} (C_{ro}C_{sa} - C_{so}C_{ra}) \mathbf{r}'_{rs} \times \int x_r \nabla x_s d\tau \quad (11)$$

(for the notation of parameters, see ref 17). The term is divided into two parts:

$$\langle \Phi_0 | \mathbf{r} \times \nabla | \Phi_a \rangle = \mathbf{R}_i \times \sum_{\text{all bonds}} (C_{ro}C_{sa} - C_{so}C_{ra}) \int x_r \nabla x_s d\tau + \sum_{\text{all bonds}} (C_{ro}C_{sa} - C_{so}C_{ra}) \mathbf{r}'_{rs} \times \int x_r \nabla x_s d\tau \quad (12)$$

where  $\mathbf{R}_i$  is the constant distance vector from the origin to the center of the chromophore, and the second term vanishes because of the symmetrical properties of the chromophores. The first term leads to eq 4 in combination with other terms. Thus the point dipole should be placed at the center of the chromophore.

- C. M. Kemp and S. F. Mason, *Tetrahedron*, **22**, 629 (1966).
- Since the present numerical calculation utilizes the observed values of transition moment  $\mu$ , excitation energy  $\sigma_0$ , and the shape of the UV spectrum of anthracene, it is, strictly speaking, a semiempirical calculation. However, the conclusion of the (6R, 15R) absolute configuration is based on the logical calculation. Therefore the present assignment holds in a nonempirical manner, irrespective of the use of semiempirical or theoretical values of these parameters.
- As depicted in Figure 4, since the two-component Cotton effects partially overlap each other, it is obvious that the peak area of the apparent Cotton effect is necessarily smaller than that of the original component Cotton effect in both cases of  $\alpha$  and  $\beta$  states. Therefore, for quantitative comparison of calculated and observed data, the observed rotational strength should be compared with the calculated apparent rotational strength, instead of the theoretical values  $R^a$  and  $R^b$  by eq 4.
- The situation is a little more complex, because even in anthracene itself, the vibronic mixing of the  $^1L_a$  transition with the  $^1B_b$  transition has been observed around 360–300 nm: J. Michl, E. W. Thulstrup, and J. H. Eggers, *Ber. Bunsenges. Phys. Chem.*, **78**, 575 (1974), and references cited therein.